URSI AP-RASC 2019, New Delhi, India; 09 - 15 March 2019

Near-field vertical coupling between terahertz photonic crystal waveguides

Daniel Headland, Xiongbin Yu, Masayuki Fujita, and Tadao Nagatsuma
Graduate School of Engineering Science, Osaka University, 1-3 Machikaneyama, 560-8531 Osaka, Japan

Abstract

We demonstrate near-field coupling between terahertz photonic crystal waveguides in the out-of-plane dimension, with no direct physical contact, by making use of coupled-line techniques. Efficient transfer (i.e. $\sim 80\%$) of terahertz power from one waveguide to another is experimentally achieved. Thereafter, multi-Gbps data is successfully transmitted via this near-field link. This study can be considered a step towards practical connectors between terahertz photonic crystal waveguide circuits.

1 Introduction

Photonic crystal waveguides composed of high-resistivity intrinsic silicon are emerging as a general-purpose platform for terahertz waves [1]. They are attractive for this purpose as the use of low-loss dielectrics engenders high efficiency, and photonic crystals provide tight confinement for compact devices. In recent years, photonic crystal waveguide circuits have been shown to hold potential for applications including terahertz sensors [2, 3], and high-volume communications [4, 5].

It is desirable to directly interface two separate terahertz photonic crystal waveguide-based circuits, as this would enable sophisticated, reconfigurable terahertz systems to be founded upon separately implemented building blocks. This manner of modularity would significantly expand the capability of the photonic crystal waveguide platform, and hence it incentivizes the development an efficient near-field connector for photonic crystal waveguides. As photonic crystal waveguide circuits are both planar and rigid, we have elected for vertical (i.e. out-of-plane) near-field coupling for this purpose, rather than side-by-side coupling, as greater interaction lengths are achievable. Whilst vertical coupling can be performed directly between photonic crystal waveguides, side-by-side coupling would likely require the assistance of structures such as bond-wires or hollow metallic waveguides, to the detriment of efficiency and cost. Furthermore, non-contact coupling is essential, as silicon is brittle, and vulnerable to breakage. Aside from connectors, this vertical-coupling capability would allow for efficient three-dimensional interconnect within terahertz photonic-crystal waveguide-based circuits. Thus, such circuits would no longer be restricted to a strictly planar structure.

Previously, we have implemented a frequency-domain diplexer in the terahertz photonic crystal waveguide platform by leveraging coupled-line techniques [6]. This is essentially a near-field connection between two waveguides that are embedded in the same silicon slab. Here, we exploit similar techniques in order to achieve efficient vertical coupling between two terahertz photonic crystal waveguides that have no physical connection between them. In order to illustrate applicability of this technique to practical systems, we demonstrate the transmission of multi-Gbps data across this near-field link.

2 Design

2.1 Waveguide

The details of the photonic crystal waveguide have previously been covered in the scientific literature [1], and hence only key details are repeated here. The photonic crystal medium consists of a triangular lattice of circular through-holes in a 200 µm-thick, high-resistivity intrinsic silicon slab. The holes are 144 µm in diameter, and spaced 240 µm apart. This produces a photonic bandgap for terahertz waves in the 300 GHz range, which prevents propagation of all in-plane modes with E-field parallel to the plane of the slab. This photonic crystal medium can therefore be considered a dielectric mirror.

If a single row of holes is omitted from the periodic structure, then this forms a line-defect along which terahertz waves are able to propagate. Thus, the defect row can be considered a terahertz waveguide. This technique has yielded highly efficient waveguides, with propagation loss below 0.1 dB/cm in the range from 326 to 331 GHz.

2.2 Coupled-line section

The structure of the coupled line section that is utilized in this work is illustrated in Fig. 1(a). Both the top and bottom lines are terahertz photonic crystal waveguides, and they are separated by vertical distance d. Coupled-line techniques depend on the existence of both odd and even modes, as illustrated in Figs. 1(b), (c), with phase constants β_{odd} and β_{even}, respectively. If one line is excited in isolation, then the field in the lines can be considered the linear superposition of these two modes [7]. Specifically, both modes have

equal magnitude, an phase such that the field in one line constructively interferes, and the other cancels out entirely. In this case, the top line is excited in this way, as illustrated in Fig. 1(d). If there were no difference in the two phase constants (i.e. $\beta_{\text{odd}} = \beta_{\text{even}}$) then these modes would propagate together, in-step, and the energy remains in the top line. However, if there is a finite difference (i.e. $\beta_{\text{odd}} \neq \beta_{\text{even}}$) then the two modes will essentially beat spatially as the wave propagates. Once a phase difference of π is accumulated between the two modes, it is as though one mode were negated with respect to the other, and hence line that previously experienced constructive interference (i.e. the top line) is now the line that experiences nullification, and vice-versa. Thus, we define the coupling length. L as the distance over which the difference in propagation constant amounts to a phase difference of π radians,

$$L = \frac{\pi}{|\beta_{\text{even}} - \beta_{\text{odd}}|}. \tag{1}$$

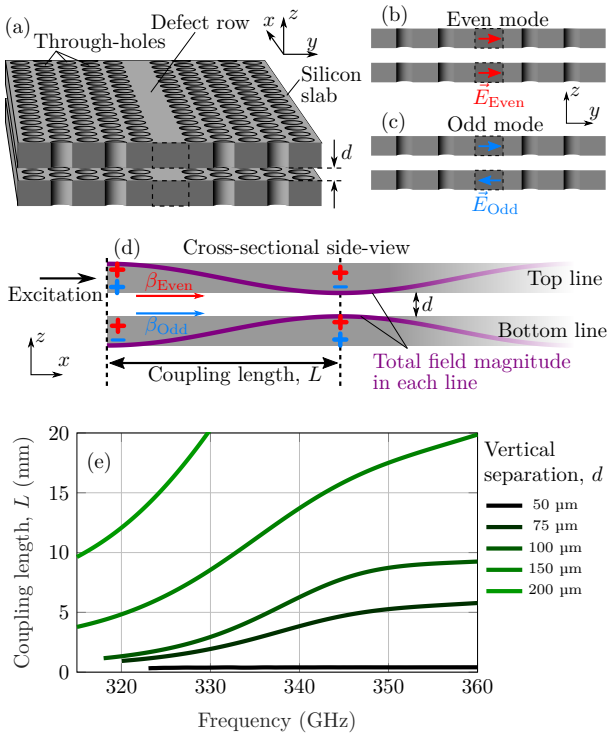

Figure 1. Coupled-line analysis, showing (a) diagram of terahertz photonic crystal waveguides in vertical coupled-line configuration, (b), (c) even and odd modes of the coupled lines, (d) illustration of the mechanism whereby terahertz power is transferred from the top line to the bottom line, and (e) results of coupled-line analysis, showing approximate theoretical coupling length as a function of frequency, for a variety of coupling lengths.

Full-wave simulations are employed in order to evaluate the approximate theoretical coupling length for a variety of vertical separations. The values of β_{odd} and β_{even} were extracted from numerical simulation as a function of frequency, for a range of vertical separations, d. The results of this procedure are given in Fig. 1(e). It can be seen that larger separation requires a longer coupling length, which is to be expected due to diminished near-field interaction. This trend continues to the extent that coupling lengths of several centimeters will be required when $d \geq 200$ µm, which is undesirable. Thus, shorter separations are preferred, to allow for practical values of coupling length. On the other hand, smaller distances render accurate positioning challenging, and carry greater risk of sample breakage. Thus, whilst the vertical separation is made as small as possible, a practical distance of ~ 100 µm is targeted.

2.3 Transition

The wave impedance of the coupled-line modes is distinct to that of a single photonic crystal waveguide in isolation, and hence a direct connection between the two forms of waveguide would generate unwanted reflections. For this reason, an anti-reflection transition between the single-line and coupled-line sections is desired in order to suppress these reflections. To this end, the photonic crystal waveguide is tapered to a spike at its termination, with the surrounding photonic crystal omitted. Thus, from the perspective of a single line, the adjacent line's width is gradually increased from zero, thereby avoiding a sudden change in wave impedance, and preventing reflection. It is found that a taper length of 3 mm, as illustrated in Fig. 2(a), is suitable for this purpose.

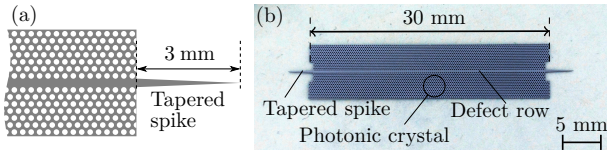

Figure 2. (a) A diagram of the tapered termination that is employed to provide gradual impedance transition, and (b) a photograph of a 3 cm-length of terahertz photonic crystal waveguide, where important features have been labelled.

3 Characterization

The waveguides were fabricated using plasma etching, and a photograph of the completed structure is shown in Fig. 2. Key features of the waveguide structure are indicated in the diagram. In order to realize the near-field coupling arrangement that is the main subject of this work, two such waveguides must be fabricated, and coupled together in the configuration that is illustrated in Fig. 3(a).

The transmission efficiency of the near-field coupling structure is probed using an all-electronic terahertz system. A millimeter-wave signal is first generated by a stable synthesiser, and then converted to the appropriate terahertz frequency by means of a $\times 9$ multiplier. Thereafter, the terahertz power is transmitted via a WR-3 hollow metallic waveguide to the top line of the near-field coupling structure. Matching between the two waveguides is achieved by inserting the photonic crystal waveguide's tapered spike

directly into the WR-3 waveguide, to provide a gradual transition. The terahertz waves then propagate through a coupled-line section, as illustrated in Fig. 3(a). Thereafter, the terahertz power that appears at the output of the bottom line is collected by a second WR-3 waveguide, and measured using a mixer. It is necessary to provide a support for the photonic crystal waveguide that allows for fine-tuning of d and L_{overlap} without interfering with the alignment between the WR-3 and photonic crystal waveguides. This is achieved by adhering each photonic crystal waveguide to a plastic structure, which is bolted directly onto the WR-3 waveguide flange.

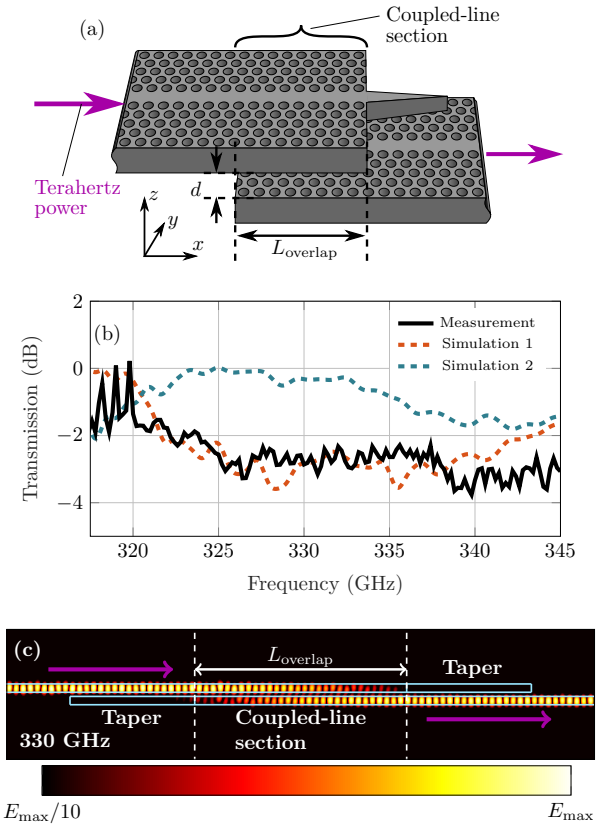

Figure 3. Characterization of the near-field coupling structure, (a) illustration of the transport of terahertz power, (b) measured and simulated transmission results, for two different parametric combinations; in both cases, $L_{\text{overlap}} = 5.1$ mm, but Simulation 1 has $d = 75$ µm, and Simulation 2 has $d = 100$ µm. A cross-sectional plot of log-scaled instantaneous field magnitude at 330 GHz is displayed in (c). Simulation 2 is selected for this purpose, as it exhibits superior performance.

The measured transmission magnitude is normalized against the transmission through a straightphotonic crystal waveguide of the same length, so as to de-embed propagation losses, as well as losses from the interface between the WR-3 and photonic crystal waveguides. The results of this procedure are given in Fig. 3(b). It can be seen that the coupling efficiency exhibits a peak of $\sim 80\%$ at around 320 GHz, although the precise value is obfuscated by significant variation. This variation is likely due to imperfect de-embedding close to the cutoff frequency of the photonic crystal waveguide's dominant mode. In the vicinity of 330 GHz, coupling efficiency is relatively stable at $\sim 50\%$.

Full-wave simulations are performed in order to compare this measured transmission to expectation. However, the precise relative positioning of the waveguides is not known explicitly, and hence a parametric investigation must be performed in order to extract the likely geometry of the measured setup. The results of this procedure are designated "Simulation 1," and plotted alongside the measured results in Fig. 3(b). In this configuration, the overlapping coupled-line section is $L_{\text{overlap}} = 5.1$ mm, and the vertical separation is $d = 75$ µm. It can be seen that reasonably-close agreement is obtained between the measured and simulated result, which is an indication that likely geometric parameters have successfully been estimated. A second simulation is performed, with a slightly larger separation of 100 µm, and the results of this simulation are also given in Fig. 3(b), as "Simulation 2." This simulation exhibits far more efficient transmission in the vicinity of 330 GHz, which shows that subtle adjustments to the geometry of this near-field coupling structure can significantly improve performance. On the other hand, the marked difference in behavior is an indication of this structure's high sensitivity to variation in the vertical separation distance.

In order to provide further insight into the vertical-coupling mechanism, a cross-sectional field plot at 330 GHz is taken from Simulation 2, and shown in Fig. 3(c). This field distribution shows the gradual transfer of energy from the top line to the bottom line, to the extent that there is no visible power remaining in the top line at the point at which it reaches the tapered section.

4 Terahertz communications

This study is largely motivated by the possibility of inter-circuit connections for practical applications of terahertz photonic crystal waveguide-based devices. In order to explore the feasibility of this aim, we incorporate this near-field-coupling technique into a demonstration of multi-Gbps communications. To this end, we make use of an optoelectronic terahertz-range communications system [5], so as to take advantage of high-speed optical modulation. A two-color laser signal is modulated, using on-off keying, with a pseudo-random binary sequence from an arbitrary waveform generator, and subsequently applied to a uni-travelling carrier photodiode (UTC-PD). This nonlinear optical component effectively extracts the beat frequency of the laser signal, which in this case is equal to 330 GHz, and transmits the generated terahertz power through a WR-3 hollow metallic waveguide. As illustrated in Fig. 4(a), a photonic crystal waveguide is coupled to the WR-3 waveguide. As before, the tapered spike is inserted directly into the hollow waveguide. Thereafter, the photonic crystal waveguide is coupled to a second photonic crystal waveg-

uide via the coupled-line section that is the main subject of this article. In this case, the length of the top line is 2 cm, and the length of the bottom line is 3 cm, as indicated in the diagram in Fig 4(a). Finally, this second photonic crystal waveguide is connected to a Schottky barrier diode (SBD) via another WR-3 waveguide. The SBD employs envelope detection in order to extracts the binary sequence, which is then routed via a limiting amplifier to a bit error rate tester in order to evaluate the quality of the terahertz link.

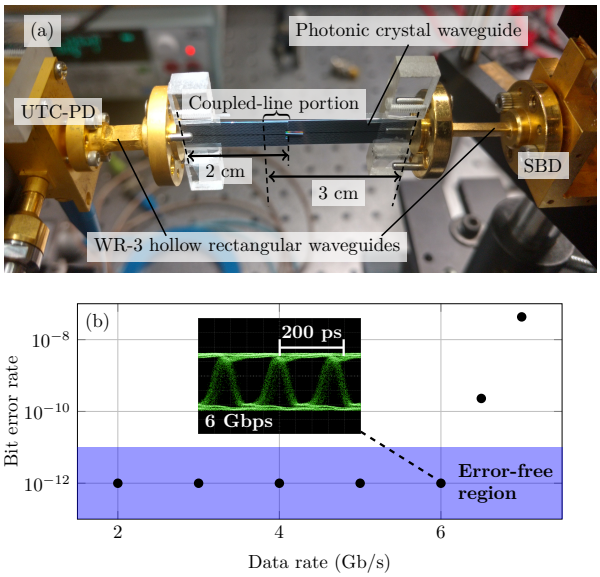

Figure 4. Demonstration of terahertz-range communications, showing (a) photograph of experimental setup, and (b) bit error rate as a function of data rate, with eye-diagram at 6 Gbps given as inset.

The bit error rate is evaluated over a range of different data rates from 2 to 7 Gbps,and results are shown in Fig. 4(b). It is noted that, from 2 to 6 Gbps, no bit errors were detected over the one-minute observation timespan. Thus, the bit error rate that is assigned to these data rates is purely nominal, and they are considered to be error-free. An eye diagram that corresponds to the maximum error-free data rate of 6 Gbps is given in the inset to Fig. 4(b), and it can be seen that the "eye" is clearly open, as is the case for reliable transmission. As the data rate is increased above 6 Gbps, the quality of the link is progressively degraded due to the finite bandwidth of the coupling structure.

5 Conclusion

We have successfully demonstrated near-field coupling between two terahertz-range photonic crystal waveguides, by leveraging coupled-line techniques. Coupling efficiency of $\sim 80\%$ is experimentally demonstrated in the vicinity of 320 GHz. Furthermore, full-wave simulations have shown that, by careful adjustment of the overlap-length and vertical separation of the two photonic crystal waveguides, the frequency of operation can be tuned, and the efficiency can be significantly increased. Multi-Gbps data was successfully transferred via this near-field link, which is an indication that it is amenable to practical applications. Thus, the near-field coupling structure is a promising candidate for a general-purpose connector between terahertz photonic crystal waveguide devices. Towards that aim, it will be necessary to develop a robust packaging structure that allows for accurate and repeatable relative positioning of the photonic crystal waveguide structures. This would also facilitate a more thorough experimental investigation into the relationship between the coupling structure's geometric parameters and coupling efficiency. This is of critical importance, as the results of this investigation have shown the near-field coupling structure to be highly sensitive to variation in vertical separation.

6 Acknowledgements

This work was supported by the Core Research for Evolutional Science and Technology (CREST) program, Japan Science and Technology Agency (JST) (JPMJCR1534), and Grant-in-Aid for Scientific Research, the Ministry of Education, Culture, Sports, Science and Technology of Japan (17H01064).

References

[1] K. Tsuruda, M. Fujita, and T. Nagatsuma, "Extremely low-loss terahertz waveguide based on silicon photonic-crystal slab," *Opt. Express*, **23**, 25, December 2015, pp. 31 977–31 990.

[2] K. Okamoto, K. Tsuruda, S. Diebold, S. Hisatake, M. Fujita, and T. Nagatsuma, "Terahertz sensor using photonic crystal cavity and resonant tunneling diodes," *J. Infrared Millim. Terahertz Waves*, **38**, 9, May 2017, pp. 1085–1097.

[3] S. Hanham, C. Watts, W. Otter, S. Lucyszyn, and N. Klein, "Dielectric measurements of nanoliter liquids with a photonic crystal resonator at terahertz frequencies," *Appl. Phys. Lett.*, **107**, 3, July 2015, art. no. 032903.

[4] W. Withayachumnankul, M. Fujita, and T. Nagatsuma, "Integrated silicon photonic crystals toward terahertz communications," *Adv. Opt. Mater.*, **6**, 16, July 2018, art. no. 1800401.

[5] W. Withayachumnankul, R. Yamada, M. Fujita, and T. Nagatsuma, "All-dielectric rod antenna array for terahertz communications," *APL Photonics*, **3**, 5, April 2018, art. no. 051707.

[6] M. Yata, M. Fujita, and T. Nagatsuma, "Photonic-crystal diplexers for terahertz-wave applications," *Opt. Express*, **24**, 7, April 2016 pp. 7835–7849.

[7] S. Boscolo, M. Midrio, and C. G. Someda, "Coupling and decoupling of electromagnetic waves in parallel 2D photonic crystal waveguides," *IEEE J. Quantum Electron.*, August 2002, **38**, 1, pp. 47–53.